Supplementary Information

Enhanced fluorescence detection of miRNA by means of Bloch surface waves-based biochips†

Agostino Occhicone,[a,b,*] Francesco Michelotti,[a,b] Paola Rosa,[a] Daniele Chiappetta,[a,b] Tommaso Pileri,[a] Paola Del Porto,[c] Norbert Danz,[d] Peter Munzert,[d] Giuseppe Pignataro,[e] and Alberto Sinibaldi[a,b]

We report on the use of biochips based on one-dimensional photonic crystals sustaining Bloch surface waves to specifically detect target miRNA that are characteristic of hemorrhagic stroke (miR-16-5p) at low concentration in a buffer solution. The biochips were functionalized with streptavidin and ssDNA oligonucleotides to enable miRNA detection. To discriminate the target miRNA from a non-specific control (miR-101a-3p), we made use of an optical platform developed to work both in label-free and fluorescence detection modes. We demonstrate that the limit of detection provided when operating in the fluorescence mode allows us to specifically detect the target miRNA down to 1ng/mL (140 pM), which matches the recommendations for diagnostic miRNA assays 5 ng/mL. The low costs open the way towards the application of these disposable optical biochips based on 1DPC sustaining Bloch surface waves as a promising tool for early disease detection in a liquid biopsy format.

S.1. The Read-out platform

In Figure S.1 a sketch of the custom-made optical read-out system is shown [1] [2] [3] [4] [5]. The integrated system is customized to integrate the optical and the fluidic components, and it acquires the signals emerging from the biochip surface working in both label-free and fluorescence operation mode. The 1DPC, complemented with its microfluidic counterpart, is mounted on the optical apparatus. During the assays, the biochip is kept at a constant temperature (T = 30°C) by means of a Peltier element, temperature fluctuations are the major sources of noise because of the thermo-optical (dependence of the refractive index on temperature) and thermo-mechanical effects.

In the LF excitation arm, the light source is a s-polarized AlGaInP laser diode (HL6756MG, Thorlabs) at λ_{LF} = 671 nm. The laser module also includes the beam shaping and collimating optics, and a rotating scatterer that destroys the spatial coherence to avoid speckles upon detection. The polarization is refined by a polarizer (POL) aligned to the TE direction, and the beam is focused onto the biochip by a cylindrical lens (CL1). In the detection arm, the illuminated line is imaged by a cylindrical Fourier lens (FL) along the long axis of a monochrome CCD camera (Apogee Ascent, Sony ICX814 chip). The illumination of a line at the surface of the biochip and accessing in a parallel manner to any spot along such a line is enabled by the cylindrical optics. The angular field of view is 2.7°, as determined by FL and the width of the CCD array (12.50 mm, 3388 pixel). The spots along the illumination line are imaged along the short axis of the CCD array (10.00 mm, 2712 pixel) by a telecentric optical system, constituted by two cylindrical lenses, S1 and S2. Such a lateral optics can image a 6 mm wide region along the illumination line with a lateral resolution below 100 µm.

In the FLUO excitation arm, the laser module includes a s-polarized laser diode at λ_{EXC} = 637 nm (L638P040, Thorlabs), a half wave plate that is used to adjust the polarization direction and an excitation filter (Chroma ZET 635/20). A cylindrical lens CL2 focuses the beam into a line at the chip surface in the same position of the LF case. The laser module can be translated by means of a motorized stage, thus tuning the average incidence angle α. The excitation beam is directed toward the biochip in an epifluorescence configuration by means of a dichroic beam splitter (DBS, Chroma ZT 640 RDC), which reflects the excitation beam and transmits the fluorescence emission. Because λ_{EM} is around λ_{LF}, it is possible to make use of the same collection optics used for the LF case. An extra zoom lens (ZOOM) was inserted in the path to increase the angular field of view to 8 deg. Furthermore, an emission filter (Chroma 655 LP ET) is placed along the path to cut stray light from the excitation beam.

[a] SAPIENZA Università di Roma, Department of Basic and Applied Sciences for Engineering, Via A. Scarpa, 16, 00161 Roma, Italy
[b] Center for Life Nano and Neuro Science, Istituto Italiano di Tecnologia (IIT), Viale Regina Elena 291, 00161 Rome, Italy.
[c] Department of Biology and Biotechnology "C. Darwin", Sapienza University of Rome, 00185 Rome, Italy.
[d] Fraunhofer Institute for Applied Optics and Precision Engineering, A.-Einstein-Str. 7, 07745 Jena, Germany.
[e] Division Pharmacology, Department of Neuroscience, School of Medicine, "Federico II" University of Naples, Italy.
*E-mail: agostino.occhicone@uniroma1.it

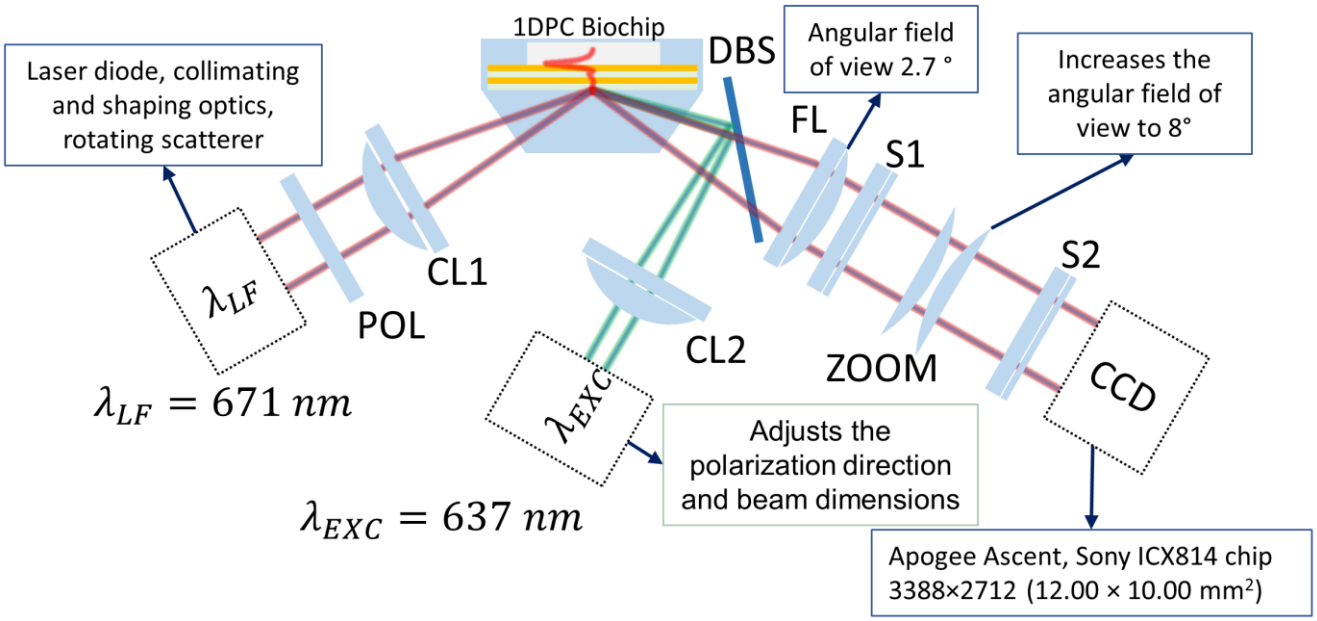

Figure S.1. Sketch of the experimental apparatus. Polarizer (POL), Cylindrical lens (CL), Fourier Lens (FL), spot imaging lenses (S1 and S2), dichroic beam splitter (DBS), zoom lenses (ZOOM).

S.2. Photobleaching

The FLUO excitation laser power used for this experiment was 32 mW (measured at the laser output) and the CCD camera integration time was fixed to $\tau = 10^{-2}\ s$. In Figure S.2, an exemplary graph of the time dependence of emission intensity during photobleaching process is shown. When the laser beam is placed to the BSW resonance position, γ_{BSW}, the I^{TE} peak decreased by a factor of about 1.5 in 5 s and by a factor 20 after 1 min. The significant decrease in fluorescence intensity is due to the overall depletion of the number of active emitters that undergo PB [3]. Thus, after 3 min almost all the emitters were photobleached. PB is typically a drawback in fluorescence measurements, but nonetheless, in this case it turned out to be a useful tool to perform the measurements.

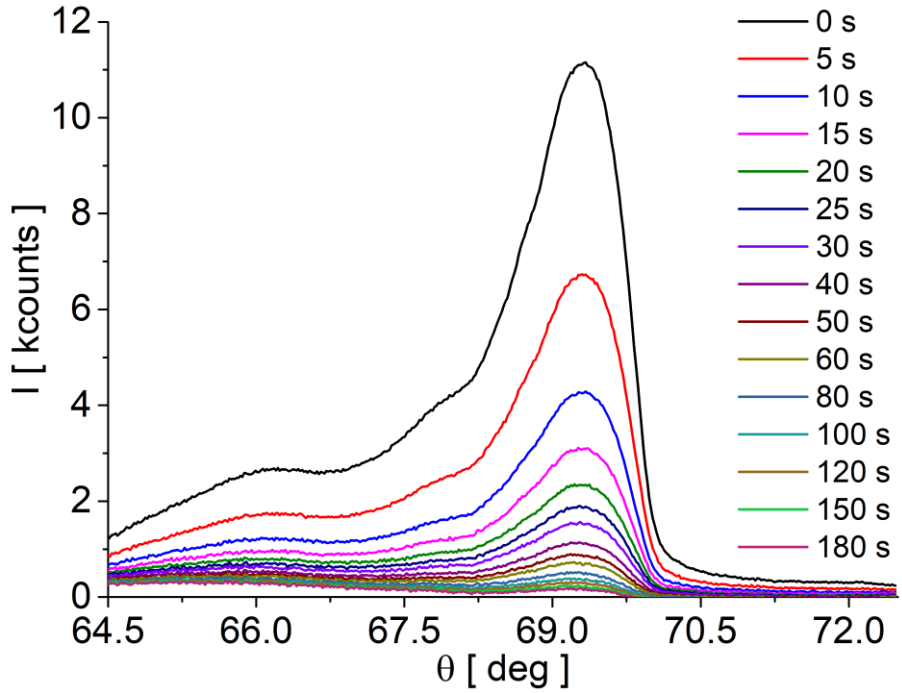

Figure S.2. Background subtracted angular fluorescence emission intensity recorded at fixed time intervals during CW FLUO excitation for Alexa Fluor 647 bound at the surface of the biochip. The curves are averaged over the signal coming from the central part of the biochip, i.e., from an area of about 2 mm wide.

S.3. Sample multiplex assay

The LF operation mode allows to detect real time θ_{BSW} sensograms and characterise the biomolecular binding processes at the surface of the biochips when the concentrations of the species are sufficiently high. We took advantage of such a possibility to set the concentrations of the C-ssDNA and D-ssDNA* to be used in the optimized assays. As an example, in Figure S.3a, we show a typical sensogram recorded during an assay carried out with a biochip whose surface was patterned as described in the main paper by means of a nanoplotter and defining 5 SIG (biotin) and 4 CTRL (BSA) zones over the biochip surface. During the assay, the LF signal was recorded in all SIG and CTRL zones. The LF residual shifts recorded in all SIG zones after all the steps of the assay are show in the bar plot of Figure S.3b. After priming of the microfluidic circuitry with PBS 1X, a regeneration solution, 20 mM glycine/HCl at pH 2.5, was used to remove non-covalently bound molecules from the surface. Because of the exposition to such a solution, a negative residual shift was recorded after the interaction (step 1). Afterwards, a solution of 20 µg/mL of streptavidin in PBS 1X was injected to selectively confer avidin properties and to define the five signal zones (SIG 1-5). As clearly shown, during the step 2 only the five biotinylated SIG zones registered a binding kinetics LF signal. Negligible residual shift was recorded in the control zones (CTRL 1-4) blocked with BSA. The biochip was then filled with sterilized water (SW) as running buffer. The biochip preparation prosecuted with the injection of a solution of C-ssDNA at a concentration of 50 µg/mL dissolved in SW (step 4). During such a step, different binding kinetics of the C-ssDNA in the SIG zones could be recorded in the LF mode, for the given C-ssDNA concentration. During the step 5, the target miRNA (rno-mi-RNA 16-5p) at a concentration of 1 µg/mL was injected and allowed to react with the biochip surface. During such a step, a partial hybridization occurred with a smaller residual LF shifts with respect to those observed in the precedent bio-conjugation steps. After a further SW washing step, the fluorescence background was acquired before injecting the fluorescent species (step 6). The miRNA recognition assay was then completed with the injection of a D-ssDNA* solution in SW at a concentration of 1 µg/mL (step 7). Such a final hybridization completed the specific pairing of the target miRNA with probe and detection oligonucleotides. The final washing procedure with SW was followed by an acquisition of the fluorescence signal (step 8).

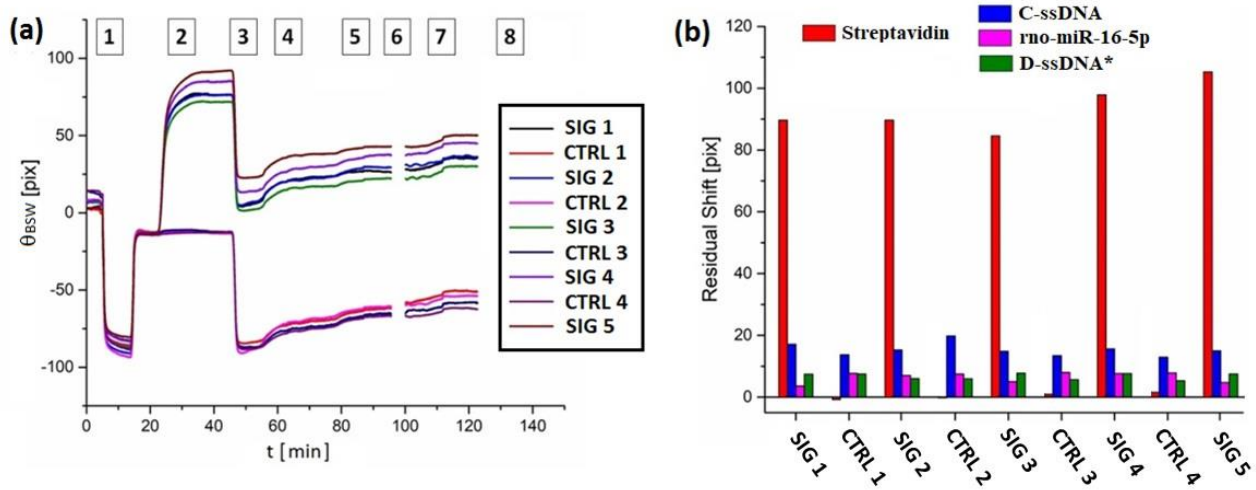

Figure S.3. (a) LF sensograms from signal (SIG 1-5) and controls (CTRL 1-4) zones; (b) histogram of the residual angular shifts after RB washing for streptavidin (red), C-ssDNA (blue), miRNA target (purple) and D-ssDNA* (green).

References

[1] Occhicone A.,Del Porto P., Danz N., Munzert P., Sinibaldi A., and Michelotti F., "Enhanced Fluorescence Detection of Interleukin 10 by Means of 1D Photonic Crystals," *Crystals,* vol. 11, no. 12, p. 1517, 2021.

[2] Rizzo R., Alvaro M., Danz N., Lucia Napione L., Descrovi E., Schmieder S., Sinibaldi A., Chandrawat Analyst i R., Rana S., Munzert P., Schuberth T., Maillart E., Anopchenko A., Rivolo P., Mascioletti A., Sonntag F., Stevens M.M., Bussolino F., and Michelotti F., "Bloch surface wave label-free and fluorescence platform for the detection of VEGF biomarker in biological matrices," *Sensors Actuators, B Chem.,* vol. 255, p. 2143–2150, 2018.

[3] Sepe E., Sinibaldi A., Danz N., Munzert P., and Michelotti F., "Anisotropic Fluorescence Emission and Photobleaching at the Surface of One-Dimensional Photonic Crystals Sustaining Bloch Surface Waves. II. Experiments," *J. Phys. Chem. C,* vol. 123, no. 34, p. 21176–21184, 2019.

[4] Sinibaldi A., Doricchi A., Pileri T., Allegretti M., Danz N., Munzert P., Giordani E., Giacomini P., and Michelotti F., "Bioassay engineering: a combined label-free and fluorescence approach to optimize HER2 detection in complex biological media," *Anal. & Bioanal. Chem.,* vol. 412, no. 14, 2020.

[5] Sinibaldi A., Sampaoli C., Danz N., Munzert P., Sonntag F., Centola F., Occhicone A., Tremante E., Giacomini P., and Michelotti F., "Bloch surface waves biosensors for high sensitivity detection of soluble ERBB2 in a complex biological environment," *Biosensors,* vol. 7, no. 3, 2017.